Variable Speed Limit Control for Freeways: A Multi-Objective Optimization Strategy Balancing Carbon Emission Reduction and Traffic Operation Efficiency

Yan Liu , Feifan Guo * , Yin Teng

Posted Date: 6 February 2026

doi: 10.20944/preprints202602.0471.v1

Keywords: travel efficiency; carbon emissions; variable speed limits; expressways; multi-objective optimization

 doi:10.20944/preprints202602.0471.v1

Article

Variable Speed Limit Control for Freeways: A Multi-Objective Optimization Strategy Balancing Carbon Emission Reduction and Traffic Operation Efficiency

Yan Liu [1], Feifan Guo [1,*] and Yin Teng [2]

[1] School of Transportation, Fujian University of Technology, Fujian 350100, China

[2] Guangxi New Development Transportation Group Co., Ltd, Guangxi 530022, China

* Correspondence: 1351017377@qq.com

Abstract

As highway traffic demand continues to rise, research on balancing carbon emissions and traffic efficiency through Variable Speed Limit (VSL) systems has become a critical topic. However, existing research has primarily focused on homogeneous road segments and connected autonomous driving scenarios, resulting in a gap in alignment with the operational requirements of actual road segments. To this end, this study focuses on heterogeneous highway sections as the core scenario. Based on the modified Greenshields model and the non-dominated sorting genetic algorithm (NSGA-II), it proposes a zoned VSL strategy optimized for dual objectives of traffic efficiency and carbon emissions. The case study results from the Qinnan section of the G75 Lanhai Expressway demonstrate that this strategy, through dynamic adjustment of speed limits, effectively enhances traffic flow stability and continuity. It achieves a synergistic increase in both traffic volume and vehicle speed while simultaneously curbing the progression of congestion during high-traffic scenarios. Additionally, this strategy achieves a cumulative reduction in carbon emissions of approximately 9.5% while maintaining traffic efficiency. It offers new insights for optimizing speed limit schemes on expressways under environmental considerations, demonstrating significant practical engineering value.

Keywords: travel efficiency; carbon emissions; variable speed limits; expressways; multi-objective optimization

1. Introduction

Changes in atmospheric conditions represent a major global challenge facing human society today. The transportation sector is not only one of the primary sources of global greenhouse gas emissions [1], but also the core source of characteristic pollutants from motor vehicle exhaust. The rapid growth of traffic demand not only leads to frequent paralysis of the transportation system, but also keeps traffic carbon emissions at a high level for a long time [2]; in particular, expressways, which are a core component of the transportation system, have their potential capacity for carbon emission optimization that cannot be ignored. Variable Speed Limit (VSL) is a technology that guides traffic flow to distribute evenly by dynamically adjusting the speed limit values for road sections: Not only does it reduce additional emissions caused by speed fluctuations, but it also enhances traffic efficiency[3]. It is now recognized as an effective means of balancing traffic operations with low-carbon emission reduction ([4,5]). In recent years, some scholars have carried out relevant research on the correlation between VSL, traffic efficiency and carbon emissions, and achieved a series of phased achievements. The VSL strategy is based on the kinematic wave theory [6], and relevant studies mostly focus on traffic congestion governance, bottleneck optimization and adaptation to complex environments: Hegyi et al. [7,8] achieved the alleviation of traffic shock waves and the reduction of travel time by combining Model Predictive Control (MPC) with VSL; Wang et al. [9]

 doi:10.20944/preprints202602.0471.v1

proposed a coordination scheme of Car-Following Control (CFC) and VSL, which improved traffic efficiency in both scenarios of manual driving and small-scale penetration of connected and autonomous driving; Li et al. [10] proposed a Q-learning-based VSL scheme that can interfere with the formation of traffic congestion in advance and avoid the decline in bottleneck capacity under fluctuating demand; Han et al. [11] made up for the defects of traffic shock waves by means of the first-order discrete MPC, and further reduced travel time. Mao et al. [12] used the Cell Transmission Model and VSL strategies to greatly reduce the duration of traffic congestion from the spatiotemporal dimension; Vrbanić et al. [13] developed the CD-QL-DPVSL algorithm, and reduced travel time through congestion area detection and dynamic adjustment of VSL areas; Fang et al. [4] adopted the multi-agent-based VSL control strategy, which effectively reduced the total waiting time at the merging bottlenecks of expressways; Li et al. [14] proposed a VSL system suitable for two-lane roads, and improved traffic efficiency by reducing the collision risk of mixed traffic flow at bottlenecks. In addition, the studies by Zhu and Ukkusuri [15], Ke et al. [16] and Han et al. [17] have also confirmed the good adaptability of VSL in complex traffic environments. In terms of carbon emission regulation, existing studies have made preliminary explorations: the VSL algorithm proposed by Khondaker et al. [18] based on MPC and the fuzzy logic VSL strategy by Coppola et al. [19] both effectively reduced vehicle fuel consumption; Roncoli et al. [20] stabilized vehicle speed within the low-emission range through the integration of multiple measures and achieved indirect emission reduction; Wu et al. [21] incorporated carbon emissions into the VSL optimization objectives and explored the multi-objective coordinated optimization strategy; Fondzenyuy et al. [22] clarified the correlation between vehicle speed control and carbon emissions through a literature review, and provided a theoretical basis for the integration of VSL and carbon emissions. In addition, Ma et al. [23] and Jin et al. ([24,25]), taking tunnel traffic as the background, confirmed the importance of considering heterogeneous road sections under the VSL strategy. These studies have laid an important foundation for solving the core problems of zonal differentiated speed limit and the coordinated optimization of carbon emissions and traffic efficiency.

Although the above studies have made certain progress, there are still many unsolved problems in the existing research on VSL strategies: (1) There is a lack of refined modeling of different speed limit values for the same road section, and most studies ignore the heterogeneity of road sections and set a unified speed limit value, which results in the lack of adaptability of speed limit schemes; (2) The integration strategies for the multi-objective optimization of carbon emissions are insufficient, and most existing achievements focus on the integration of traffic efficiency and safety or single-objective optimization. (3) The developed models lack consideration of actual road parameters, parameter calibration deviates from reality, and most of them rely on simplified traffic flow models and emission models [26,27], which leads to deviations between theoretical models and actual engineering practices; (4) The weight balance in multi-objective solution is not perfect, and most existing studies mostly adopt fixed weights to handle objectives of different dimensions, making it difficult to adjust the priority of carbon emissions and traffic efficiency according to dynamic traffic scenarios [28,29]. Therefore, to better align with the actual operation environments and decision-making scenarios of expressways, this study addresses the above shortcomings, takes heterogeneous elements such as road alignment, longitudinal gradient, bridges and tunnels as constraint conditions, takes the zonal variable speed limit of expressways as the regulation measure, carries out scenario-based upgrading based on the modified Greenshields model and the NSGA-II algorithm, and establishes a dual-objective optimization strategy for traffic efficiency and carbon emissions by combining actual road parameters.

2. Materials and Methods

2.1. Analysis of Impacts on Traffic Operation Efficiency and Carbon Emissions Under Zonal VSL

VSL relies on the integrated application of technologies such as electronic control, data communication and computer processing, dynamically sets the speed limit values for each speed

 doi:10.20944/preprints202602.0471.v1

limit subzone, and achieves real-time regulation of vehicle travel speed by pushing this information to drivers. Assuming that the expressway variable speed limit system is divided into n speed limit subzones, its typical control structure is shown in Figure 1: Detector i is deployed at the connection section between Subzone i and Subzone i+1 to collect the traffic operation data of Subzone i; Variable Message Sign i is installed at the end of Subzone i to issue the variable speed limit instructions for Subzone i+1.

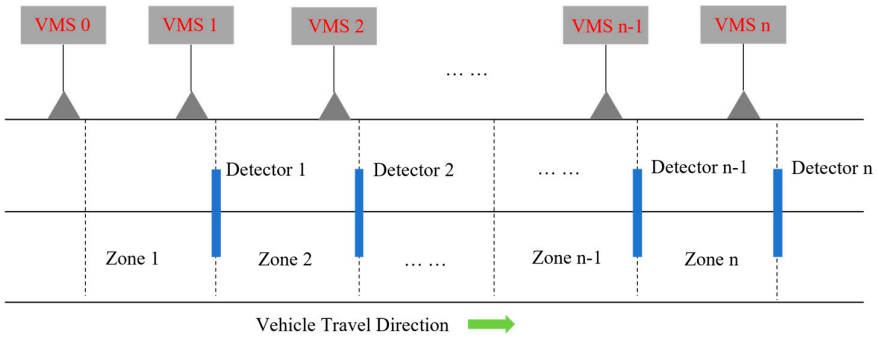

Figure 1. Typical variable speed limit control (VSL) structure.

The action mechanism of VSL in the fundamental diagram of traffic flow depends on the traffic flow model. As shown in Figure 2, according to the variation law of the fundamental diagram of traffic flow, under the unrestricted speed condition, the traffic state will quickly enter the congestion phase when the traffic density exceeds the critical density k_c. Adjusting the speed limit values can change the fundamental characteristics of traffic flow, and under the working conditions with high congestion risk, a lower speed limit value is set to prevent road sections from entering the congestion state prematurely. In addition, after the implementation of VSL, the critical density can be increased to k_c^1, k_c^2, which means that a stable traffic flow can still be maintained at a higher critical density. For this reason, we draw a conclusion: VSL can directly regulate the average travel speed of road sections, and on this basis, drive the traffic operation state of road sections by indirectly affecting the traffic flow and traffic density, so as to achieve the homogenization of traffic flow and the alleviation of traffic congestion.

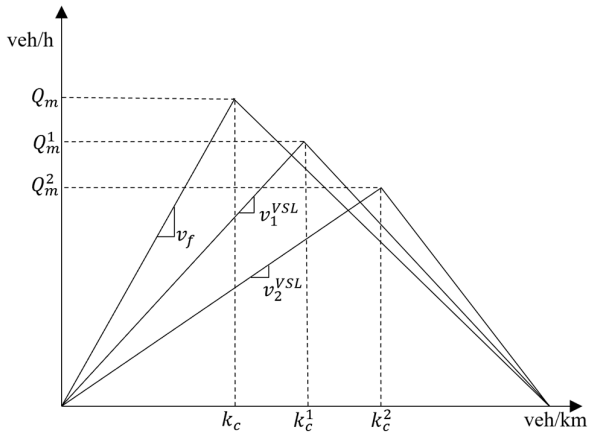

Figure 2. The influence of VSL on the fundamental diagram of traffic flow.

VSL can effectively alleviate the travel delay on expressway bottleneck road sections (Figure 3): the enclosed area by the cumulative vehicle arrival curve and the bottleneck passage rate curve in the figure corresponds to the total system delay; the capacity of bottleneck road sections is q_d under the

 doi:10.20944/preprints202602.0471.v1

uncontrolled working condition, while VSL can regulate the bottleneck traffic flow to $q_A(q_A > q_d)$, thereby avoiding the decline of road section capacity, eliminating bottleneck congestion, and at the same time reducing the scope of the area corresponding to total delay to achieve a reduction in the overall delay of road sections. It should be noted that the speed limit values of variable speed limit must be maintained within a reasonable range and must not exceed the maximum traffic flow value of speed limit subzones. If this value is exceeded, the bottleneck passage rate will not be able to be stably maintained at the q_A level, and the control measures will fail to achieve the expected delay reduction effect.

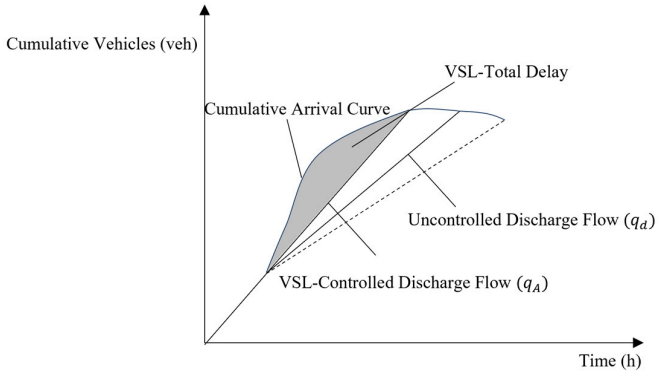

Figure 3. The influence of VSL on travel delay.

Vehicle speed dispersion has a significant impact on vehicle carbon emissions [30,31]. Within the statutory speed limit range, vehicle carbon emission levels show significant nonlinear correlation characteristics with the change of speed limit values, and this rule provides core theoretical support for the construction of VSL multi-objective optimization schemes. The dual-objective optimization model constructed later in this study is precisely based on this nonlinear relationship. It regulates the speed limit values within a reasonable range, which not only improves road traffic efficiency by increasing traffic flow, but also effectively avoids the problem of a sharp increase in carbon emissions caused by improper speed limit setting, and ultimately achieves the coordinated optimization objective of improving traffic efficiency and reducing carbon emissions.

2.2. Data Sources

This study selects the Qinnan Section of Lan-Hai Expressway G75 as the research object. This section has a total length of 138.48 km, including 57 horizontal curves with a minimum radius of 1 km and the longest straight section of 3.95 km, with horizontal curves accounting for 55.6% of the total length. It is equipped with 101 grade change points and has a maximum longitudinal gradient of 3.227%. The actual traffic flow data were obtained from the three consecutive days of traffic flow data from February 26 to 28, 2023 on the Guangxi Smart Expressway Cloud Control Platform. This data covers the monitoring information of 3 first-class traffic survey stations and 2 second-class traffic survey stations, with a total traffic volume of 858,310 vehicle trips recorded. Through the Paramics simulation platform, the vehicle operation process of the Qinnan Section of G75 Lan-Hai Expressway from February 26 to 28, 2023 was simulated, and the Monitor module was used to collect vehicle exhaust emission data. In addition, this study divided the road section into 3 variable speed limit subzones, and determined the basic road parameters of the section by consulting the construction design drawings and approval documents of the section:

1. Subzone 1 (20 km): including 15 horizontal curves with a minimum radius of 1 km and a maximum straight section length of 1.836 km, with a horizontal curve ratio of 63.6%; it has a maximum longitudinal gradient of 1.85%, a minimum slope length of 521 m and a vertical curve

 doi:10.20944/preprints202602.0471.v1

ratio of 46.34%, among which the convex vertical curve has a minimum radius of 18 km and the concave vertical curve has a minimum radius of 12.15 km.

2. Subzone 2 (5 km): including the longest Tieshan Port Cross-sea Bridge in Guangxi, with a bridge length of 2.898 km and a deck width of 26.5 m. The bridge crosses Tieshan Port and connects the G75 Yuzhan Expressway and the Lan-Hai Expressway.
3. Subzone 3 (25 km): including 7 horizontal curves with a minimum radius of 1.5 km and a maximum straight section length of 3.332 km, with a horizontal curve ratio of 60.23%; it has a maximum longitudinal gradient of 2.219%, a minimum slope length of 0.502 km and a vertical curve ratio of 56.388%, among which the convex vertical curve has a minimum radius of 11 km and the concave vertical curve has a minimum radius of 12 km.

2.3. Data Processing

This dataset contains more than 850,000 traffic records, covering vehicle types such as small and medium-sized passenger cars, large passenger cars and various types of freight trucks, and involving parameters such as vehicle speed, traffic volume and congestion degree. There are abnormal and missing phenomena in the data, such as a vehicle speed of 0 and negative traffic volume. Based on the characteristics of time series, this study adopts the linear interpolation method to process the missing values of vehicle speed, and eliminates invalid characters and marks at the same time to ensure the standardization of the numerical format of the data. For abnormal values, if direct removal is adopted for all of them, problems such as insufficient data and changes in data distribution may occur. For this reason, the direct deletion method is adopted for abnormal values caused by data entry errors, incorrect device reports and other such reasons, while the mean value replacement method of adjacent time periods is adopted for abnormal values caused by emergencies such as traffic accidents. After the above processing, a total of 124,067 valid vehicle trip data were retained. To focus on the dual-objective optimization problem of macroscopic carbon emissions and traffic efficiency of each subzone under VSL, all vehicle types are uniformly converted into standard passenger car equivalents in accordance with the *Technical Standard for Highway Engineering* (JTG B01-2014) (Table 1):

Table 1. Representative vehicle types and conversion coefficients.

Representative vehicle type	Conversion coefficient	Description
Small passenger car	1.0	Seats≤ 19，Cargo capacity≤2t
Medium-sized vehicle	1.5	Seats＞19，2t<Cargo capacity≤7t
Large vehicle	2.5	7t< Cargo capacity≤ 20t
Tractor-trailer	4.0	Cargo capacity＞20t

Meanwhile, to meet the analysis requirements of the time-varying characteristics of traffic flow, hourly aggregation processing was performed on the screened data, finally generating 144 sets of valid hourly data. During the simulation data collection process, abnormal values are prone to appear in the data due to the influence of factors such as improper parameter setting, distorted boundary conditions and numerical calculation errors. Such abnormal values will seriously interfere with the accuracy and reliability of subsequent data analysis, so it is crucial to conduct abnormal value detection in the data preprocessing stage. This study adopts the box plot method for the abnormal value detection of simulation data. As shown in Figure 4, taking the vehicle speed data of a certain time series as an example, this data reflects the average vehicle speed over a period of time. The results show that most of the vehicle speed data is concentrated in the reasonable range above 80 km/h, while the detected abnormal values are mostly distributed in the range above 100 km/h.

 doi:10.20944/preprints202602.0471.v1

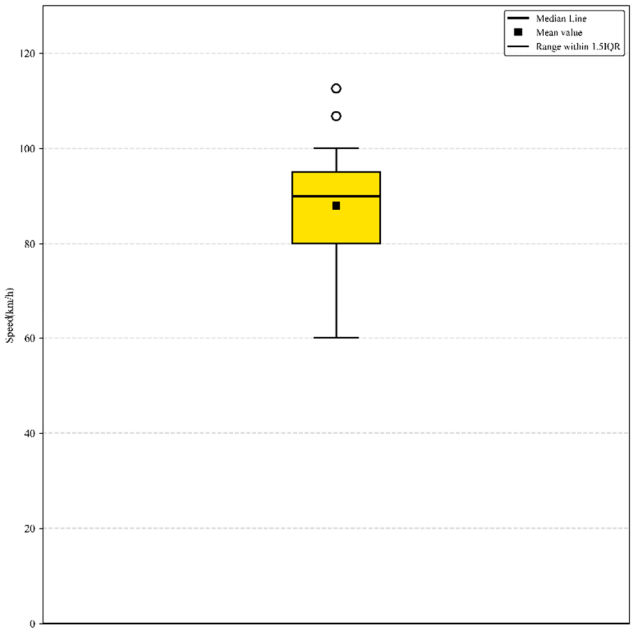

Figure 4. Abnormal value detection.

2.4. Data Analysis

This study takes the three consecutive days of traffic flow data under the fixed speed limit mode on the Qinnan Section of G75 Expressway from February 26 to 28, 2023 as the sample. After processing, this sample includes various indicators such as average vehicle speed, equivalent traffic volume and congestion index. The traffic flow characteristics of the expressway under the fixed speed limit mode are explained through time series analysis (Figure 5):

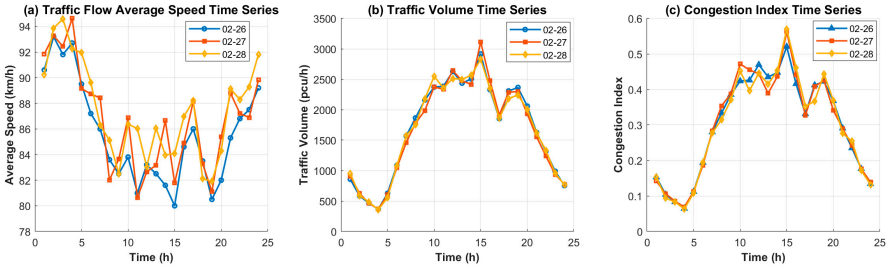

Figure 5. Traffic flow characteristics under the fixed speed limit mode.

From the multi-indicator characteristics in Figure 5, vehicle speed shows significant fluctuation characteristics under the fixed speed limit condition: especially during the period from 9:00 to 10:00 on the 28th, the maximum fluctuation range reaches 6 km/h. Meanwhile, the congestion index also presents the same variation trend, and higher traffic demand will further amplify such instability. In addition, during the period of rising traffic volume, vehicle speed not only failed to increase synchronously, but also experienced a reverse decline on many occasions. It can be seen that the rigid constraints of the fixed speed limit mode not only lead to traffic flow disorder and increase the difficulty of congestion pre-control, but also reflect its weak adaptability to scenarios with high traffic demand. To explore the correlation between vehicle speed and carbon emission rate, this study conducts simulation experiments based on the actual vehicle operation conditions of the study section. During the simulation process, the standardized method is still adopted to uniformly convert all vehicle types into passenger car units (PCU), and data cluster analysis at the hourly level is carried out, finally generating a time-series data sequence containing average vehicle speed and carbon

 doi:10.20944/preprints202602.0471.v1

emission rate. Figure 6 illustrates the U-shaped nonlinear correlation between vehicle speed and carbon emission rate. This pattern depicts the dynamic corresponding relationship between vehicle speed fluctuations and carbon emission characteristics, and provides data support for the subsequent quantitative analysis of the internal interaction mechanism between the two.

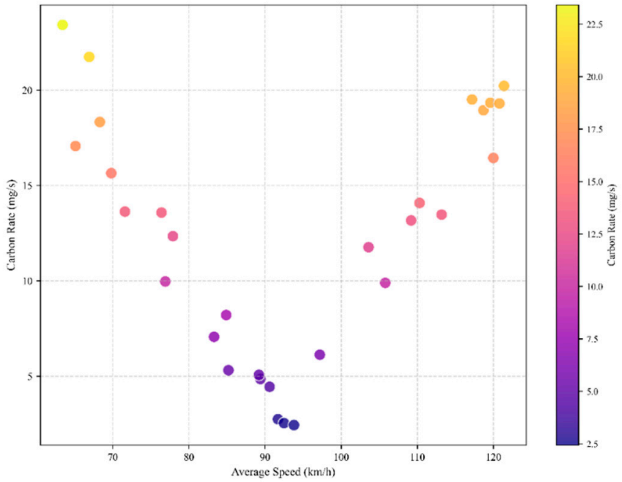

Figure 6. Correlation characteristics between vehicle speed and carbon emission rate.

2.5. Construction of Optimization Functions

Based on the classic traffic flow model, this study accomplished the scenario-based adaptive upgrading of the model through fitting and calibration with actual data and the embedding of targeted constraint conditions. Meanwhile, the NSGA-II algorithm is adopted as the solution framework for the multi-objective optimization function system, anchoring the research focus on the optimization problems in actual engineering scenarios.

2.5.1. Objective Function

During the solution process of the multi-objective function, this study adopts the min-max standardization method to perform dimension unification processing on each objective function, so as to balance the weight relationships among the objective functions and determine the function value coefficients.

$$f_1' = \frac{f_1 - f_{1min}}{f_{1max} - f_{1min}} \quad (1)$$

$$f_2' = \frac{f_2 - f_{2min}}{f_{2max} - f_{2min}} \quad (2)$$

$$f_3' = \frac{f_3 - f_{3min}}{f_{3max} - f_{3min}} \quad (3)$$

Final objective function is:

$$min\, F = f_1' - f_2' + f_3' \quad (4)$$

Where f_1 is the carbon emission optimization objective function, f_2 is the traffic flow optimization objective function, and f_3 is the travel time optimization objective function.

2.5.2. Carbon Emission Optimization Function

Combined with the operational characteristics of traffic flow and the internal interaction mechanism of motor vehicle pollutant emissions, this study adopts the data fitting method to establish a functional correlation model between average vehicle speed and carbon emission rate.

$$Y(v_i) = a_1 v_i^2 + a_2 v_i + a_3 \quad (5)$$

Where a_1, a_2, and a_3 are fitting coefficients calibrated with field data.

 doi:10.20944/preprints202602.0471.v1

Further considering the spatial division characteristics of the road section, the length of each subzone within the study section is set as L_i, and the functional relationship between the average vehicle speed v_i of each subzone and its carbon emission $Y(v_i)$ is derived:

$$P(v_i) = \frac{L_i Y(v_i)}{v_i} = L_i \left(a_1 v_1 + \frac{a_2}{v_i} + a_3\right) \quad (6)$$

The vehicle operation process on the Qinnan Section of G75 Lanhai Expressway was simulated using the Paramics simulation platform, and exhaust emission data was collected with the software's built-in Monitor module. After data preprocessing, the average vehicle speed of vehicles and the corresponding emission rate data of carbon monoxide (CO) and hydrocarbons (HC) were extracted. Regression fitting analysis was conducted on the average vehicle speed and carbon emission rate (defined as the sum of the CO emission rate and HC emission rate), with the fitting results shown in Figure 7:

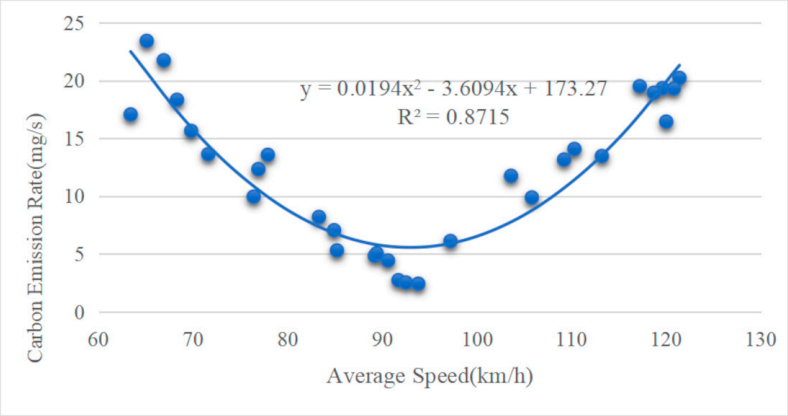

Figure 7. Fitting results of carbon emission rate and average vehicle speed.

The coefficient of determination of this fitting is R^2=0.8715, which indicates a high matching degree between the fitted values and the measured values, and the constructed fitting model can effectively characterize the quantitative correlation between the carbon emission rate and the average vehicle speed. Based on this, the functional relationship formula between the average vehicle speed and the carbon emission rate is determined:

$$Y(v_i) = 0.0194 v_i^2 - 3.6094 v_i + 173.27 \quad (7)$$

Meanwhile, the quantitative functional correlation model between the average vehicle speed and carbon emissions is obtained:

$$P(v_i) = \frac{L_i Y(v_i)}{v_i} = L_i \left(0.0194 v_i + \frac{173.27}{v_i} - 3.6094\right) \quad (8)$$

Based on the fact that the speed limit is generally higher than the average vehicle speed, let the speed limit of speed limit subzone i be V_i, then we have:

$$v_i = \lambda V_i \quad (9)$$

The introduced reduction coefficient λ is determined by comparing the actual average vehicle speed with the speed limit value (Table 2), and its calibration is accomplished through the fitting method based on field observation data.

Table 2. Reduction coefficients under different speed limit conditions.

speed limit value (km/h)	70	80	90	100	110	120
λ	0.93	0.87	0.85	0.84	0.82	0.77

Finally, the carbon emission rate optimization model for the entire variable speed limit control area is obtained:

 doi:10.20944/preprints202602.0471.v1

$$f_1(V) = \sum_{i=1}^{n} P(V_i) \quad (10)$$

$$P(V_i) = L_i\left(0.0194\lambda V_i + \frac{173.27}{\lambda V_i} - 3.6094\right) \quad (11)$$

2.5.3. Traffic Flow Optimization Function

To establish the traffic flow optimization function for highway sections, this study takes the Greenshields model as the theoretical support. In view of the inherent limitations of the original model in depicting the evolution law of actual traffic flow on highways, targeted revisions are further made to it to improve the authenticity and accuracy of traffic flow characterization:

$$Q(v_i) = \begin{cases} \rho_j\left(v_i - \frac{v_i^2}{v_f}\right) & , v \geq v_m \\ k_1 v_i^2 + k_2 v_i + k_3 & , 0 \leq v \leq v_m \end{cases} \quad (12)$$

Where ρ_j is the blocking density, v_f the free-flow speed, v_m the optimal speed, and k_1, k_2, k_3 the fitting coefficients. The traffic flow optimization function for highways constructed in this study is shown in the following formula:

$$f_2(V) = \sum_{i=1}^{n} Q(V_i) \quad (13)$$

$$Q(V_i) = \begin{cases} \rho_j\left(\lambda V_i - \frac{(\lambda V_i)^2}{v_f}\right) & , \lambda V_i \geq v_m \\ k_1(\lambda V_i)^2 + k_2\lambda V_i + k_3 & , 0 \leq \lambda V_i \leq v_m \end{cases} \quad (14)$$

k_1, k_2 and k_3 are key fitting coefficients characterizing the road congestion state. This study conducts parameter fitting based on the measured traffic flow data of the Qinnan Section of the G75 Lanhai Expressway, with the minimization of fitting residuals and the maximization of R^2 as the core evaluation criteria. The optimal combination of fitting coefficients is screened out and substituted into the subsequent research models. The fitting results are shown in Figure 8:

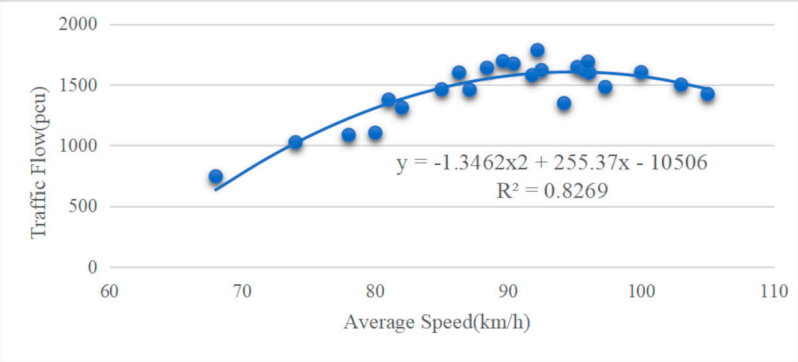

Figure 8. Fitting results of traffic flow and average speed.

The R^2 of this fitting is 0.8269, indicating the reliability of the fitting results. Based on the quantitative relationship between the speed limit value and the actual average vehicle speed established above, the correlation model between traffic flow and speed limit value in the speed limit subzone is finally obtained:

$$Q(V_i) = \begin{cases} \rho_j\left(\lambda V_i - \frac{(\lambda V_i)^2}{v_f}\right) & , \lambda V_i \geq v_m \\ -1.13462(\lambda V_i)^2 + 255.37\lambda V_i - 10506 & , 0 \leq \lambda V_i \leq v_m \end{cases} \quad (15)$$

2.5.4. Travel Time Optimization Function

Given that the section length of variable speed limit subzone i is L_i, the average travel time $T(v_i)$ of vehicles within the subzone is given by:

$$T(v_i) = \frac{L_i}{v_i} \quad (16)$$

 doi:10.20944/preprints202602.0471.v1

Combined with the relationship between the speed limit value and the average vehicle speed, the travel time optimization function for the entire variable speed limit subzone is as follows:

$f_3(V) = \sum_{i=1}^{n} \frac{L_i}{\lambda V_i}$ (17)

2.5.5. Constraints

Considering the actual traffic operation characteristics of highways, to avoid traffic flow disturbances caused by abrupt changes in speed limits on adjacent road sections, this study establishes a coordinated speed limit constraint: the absolute difference in speed limits between adjacent road sections in the same time period shall not exceed 20 km/h.

$|V_i - V_{i+1}| \leq 20km/h$ (18)

Where V_i is the speed limit value and set as a discrete integer.

When vehicles travel on curved sections of highways, an excessively high driving speed will damage the vehicle's lateral dynamic balance and thus induce rollover accidents. To ensure traffic safety on curved sections, this study imposes the following constraints on the speed limit values of the sections based on the geometric alignment characteristics of curved roads:

$V_{imax} = V_i \leq \sqrt{127R_{imin}(\varphi_{hmax} + i_{hmax})}$ (19)

Where R_{imin} is the minimum curve radius of variable speed limit subzone i; i_h is the pavement cross slope; φ_h is the transverse adhesion coefficient, which is generally taken as 0.6~0.7.

In accordance with the technical requirements of the *Technical Standard for Highway Engineering* (JTG B01-2014), the maximum longitudinal slope limits of roads show significant differences with the variation of design speed, and there is a clear corresponding relationship between the two. To ensure the stability and safety of vehicle driving on longitudinal slope sections, and avoid driving risks caused by excessive or abrupt longitudinal slopes, this study incorporates road longitudinal slope into the constraint system for variable speed limit control. The specific constraint indicators are shown in Table 3.

Table 3. Maximum longitudinal slope limits.

Design speed (km/h)	60	80	100	120
Maximum longitudinal slope (%)	6	5	4	3

3. Results

3.1. Algorithm Solution and Analysis

This study introduces the NSGA-II algorithm as the solution framework for the multi-objective optimization problem. This algorithm can effectively balance the convergence and distribution of solutions and generate a uniformly distributed Pareto optimal front. In view of the three mutually restrictive objective functions in the constructed highway variable speed limit control model, to simplify the calculation process of algorithm solution and reduce the computational complexity, the objective functions are equivalently reconstructed in the iterative solution stage: $\max f_2$ is defined as $f_1(x_i)$, and the sum of $\min f_1$ and $\min f_3$ is defined as $f_2(x_i)$.

The NSGA-II algorithm is adopted to solve the reconstructed bi-objective optimization model, and its dominance relationship is defined as:

$$x_i \prec x_j \Leftrightarrow \left(\forall m \in \{1,2\}, f_m(x_i) \leq f_m(x_j)\right) \wedge \left(\exists m \in \{1,2\}, f_m(x_i) < f_m(x_j)\right) \quad (20)$$

In the formula, m corresponds to the number of reconstructed objective functions, and $x_i = [V_1, V_2, V_3]$、$x_j = [V_1', V_2', V_3']$ are the scheme vectors containing the speed limit values of the three subzones.

 doi:10.20944/preprints202602.0471.v1

Regarding dominance count and non-dominance rank assignment, they are the core indicators of the fast non-dominated sorting in NSGA-II:

$$n(x) = |\{ y \in P \mid y \prec x \}| \tag{21}$$

$$F_1 = \{ x \in P \mid n(x) = 0 \}, F_{k+1} = \left\{ y \in P \setminus \bigcup_{i=1}^{k} F_i \mid n(y) = 0 \right\} \tag{22}$$

Where the judgment of $y \prec x$ is based on the reconstructed $f_1(x)$ and $f_2(x)$; F_1 is the Pareto front for the bi-objective problem, from which the optimal speed limit schemes are selected. The crowding distance calculation of NSGA-II is adopted to maintain the diversity of solutions:

$$I(x) = \sum_{m=1}^{2} \frac{f_m(x_{m+1}) - f_m(x_{m-1})}{f_m^{\max}(F_k) - f_m^{\min}(F_k)} \tag{23}$$

Where $f_1^{\max\text{-}\min}(F_k)$、$f_2^{\max\text{-}\min}(F_k)$ are the extreme values of the traffic flow objective and the carbon emission + travel time objective in the k level non-dominated solutions, respectively. It is assumed that the boundary individuals have $I(x) = \infty$ to ensure their priority in selection. Finally, the crowding comparison operator is adopted for the selection of the next-generation population.

$$x \succ_{\text{crowd}} y \Leftrightarrow \left(\text{rank}(x) < \text{rank}(y)\right) \vee \left(\text{rank}(x) = \text{rank}(y) \wedge I(x) > I(y)\right) \tag{24}$$

Where x and y both refer to two different individuals of speed limit schemes in the population, and $\text{rank}(x)$ is the non-dominated rank of individual x (the rank of F_1 is 1). Based on this operator, 250 individuals are selected from the merged population, and the iteration is terminated after 500 iterations.

The basic road parameters of the study section are substituted into the optimization model, and the following parameters are selected as the input parameters of the NSGA-II algorithm (Table 4):

Table 4. Algorithm parameter settings.

Parameter	Numerical value
Population size	250
Number of iterations	500
Objective function	2
Dimension	3
Crossover probability	0.9
Distribution index of crossover and mutation algorithm	0.02

To verify the effectiveness of the bi-objective optimization model in the traffic flow and carbon emission control of highways, this study completes the verification through the convergence of the objective function, the analysis of dynamic regulation of zonal speed limits and the visualization of Pareto optimal solutions. Figure (a) shows that the algorithm effectively explores the global feasible region of the objective functions at the initial stage of iteration, and all objective functions tend to a stable convergent state after 200 iterations. Figure (b) further reveals the driving effect of the dynamic regulation of zonal speed limits on the convergence of the objective functions, with the two having exactly the same convergence timing. The Pareto optimal solutions presented in Figure (c) clearly define the non-dominated solution boundary for traffic flow and carbon emissions, which verifies the rationality of the model solutions from the perspective of optimization results. The optimal speed limits for each subzone are finally determined as 90 km/h, 80 km/h and 100 km/h. The NSGA-II algorithm, which serves as the solution framework for this multi-objective optimization problem, not only features a fast convergence speed and stable solution performance, but also can achieve

 doi:10.20944/preprints202602.0471.v1

differentiated regulation of zonal speed limits and multi-objective collaborative optimization based on the differences in traffic characteristics and road conditions of each subzone.

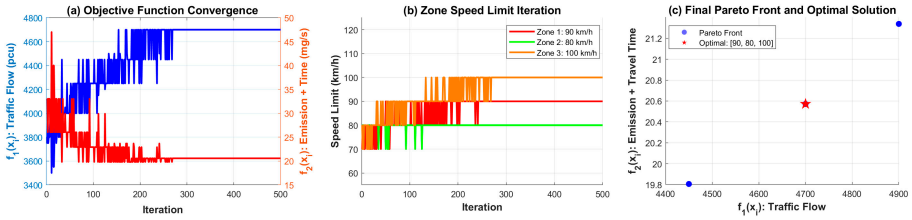

Figure 9. Iteration process of NSGA-II multi-objective optimization.

In the verification stage, to further test the practical application effectiveness of the proposed model, the above optimal speed limit scheme is applied to the target study section. Continuous 24-hour traffic flow monitoring is carried out for the upward and downward directions of the section, with core parameter data such as vehicle speed and traffic volume collected. After standardized screening and processing, 48 groups of valid hourly data samples are finally determined. It can be seen from the verification results in Figure 10 that, compared with the traffic operation characteristics of highways under the traditional fixed speed limit mode, the zonal VSL strategy, by dynamically regulating the speed limit values of road sections, not only effectively balances the speed dispersion within the sections and enhances the stability and continuity of traffic flow operation, but also breaks through the rigid constraints of fixed speed limits, realizing the coordinated positive correlation development of traffic volume and driving speed, and at the same time can effectively control the risk of traffic congestion evolution under high-traffic scenarios.

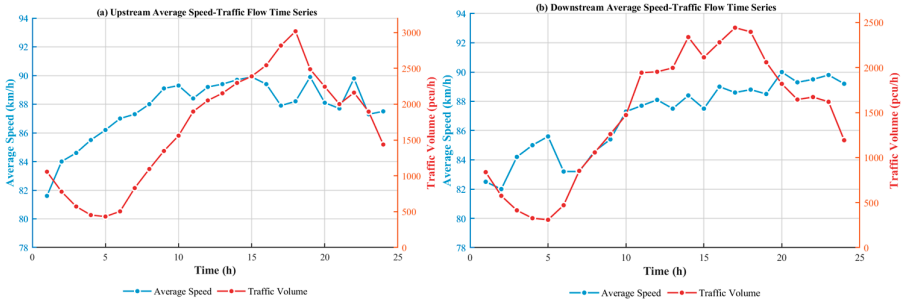

Figure 10. Traffic flow characteristics under zonal VSL.

To clearly characterize the differentiated carbon emission features of each subzone, this study selects the traffic flow data of the upward direction of the sample section as the baseline data, compares and verifies the changes in vehicle carbon emissions before and after the implementation of the VSL strategy, and conducts the analysis with the carbon emissions generated by a single vehicle passing through each subzone in full as the accounting benchmark. It can be seen from the verification results in Figure 11 that after the implementation of the zonal VSL strategy, all three subzones have achieved significant carbon emission reduction effects: Subzone 1 has a reduction rate of 4.1%, Subzone 2 11.6%, and Subzone 3 has the best emission reduction effect, reaching 13.2%. By dynamically regulating the speed limit values of the highway, this strategy effectively avoids the severe fluctuations in vehicle speed and low-efficiency engine operating conditions that are likely to occur in high-traffic scenarios under the traditional fixed speed limit mode, optimizes the overall driving state of vehicles, and thus achieves a steady drop in carbon emissions.

 doi:10.20944/preprints202602.0471.v1

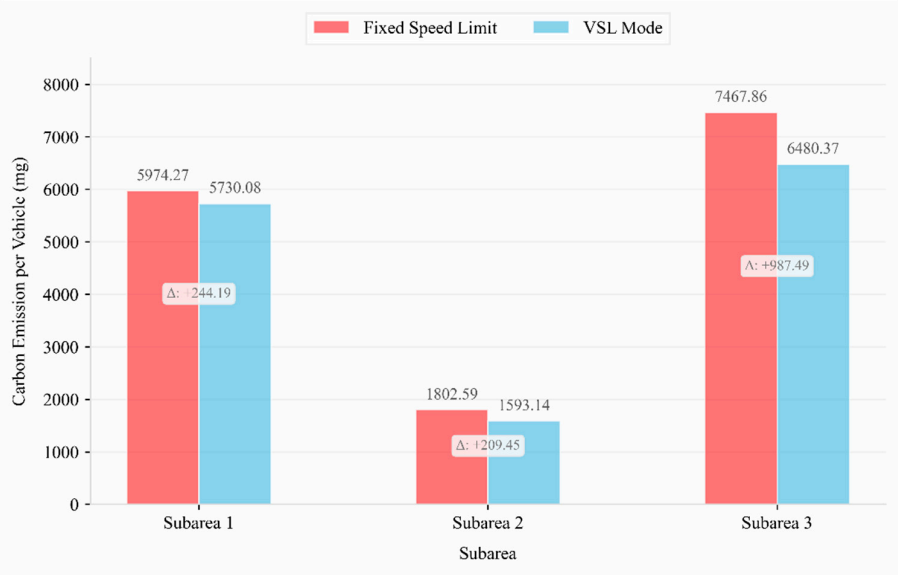

Figure 11. Comparison of per-vehicle carbon emission modes in each subzone.

4. Discussion

To address the problems in existing highway VSL research, such as insufficient collaborative optimization of traffic efficiency and vehicle carbon emissions, overemphasis on single homogeneous road sections while neglecting heterogeneous characteristics, and poor adaptability in actual operation scenarios, this study takes the Qinnan Section of Lan-Hai Expressway G75 as the case scenario and proposes a multi-objective optimization strategy based on the modified Greenshields model and NSGA-II algorithm. Relying on actual traffic flow monitoring data and Paramics simulation data, it incorporates heterogeneous elements including differences between main lines and bridge-tunnel sections, speed differences of adjacent road sections, horizontal curve parameters and longitudinal gradients into the constraint system, and establishes a multi-objective function for carbon emissions, traffic volume and travel time, thus realizing the effective optimization of VSL for heterogeneous highway sections. Meanwhile, this study takes the NSGA-II algorithm as the solution framework for the multi-objective optimization problem. Through min-max standardization and Pareto optimal solution screening, it effectively addresses the problems of dimension unification and imbalanced weight distribution in multi-objective optimization, verifies the rationality of the model solutions from the perspective of optimization results, and improves the engineering practicability of the scheme. Through controlled comparative verification, the optimization strategy proposed in this study can achieve an effective balance in the mechanistic correlation between vehicle carbon emissions and traffic efficiency on highways. It reveals that under the VSL mode, the steady reduction in vehicle carbon emissions does not depend on changes in traffic volume, but is a direct effect of the dynamic regulation of vehicle speed. It also further clarifies the differences in emission reduction potential among different subzones within the same road section. However, this study mainly explores the synergistic optimization effect of traffic efficiency and carbon emissions under the zonal VSL strategy for highways from a macro perspective. Future research can focus on the driving characteristics and emission differences of different vehicle types (including new energy vehicles), refine the dynamic deployment scheme of the zonal VSL system, and improve the adaptation accuracy of the strategy to vehicle type heterogeneity. In addition, the current research focuses on the optimization scenario of a single road section with multiple subzones. Future research can expand the research dimension to the road network scale, further investigate the synergistic regulation mechanism of VSL for adjacent road sections and interchange nodes, and avoid the problem of traffic bottleneck transfer that may be caused by the regulation of a single road section through systematic

 doi:10.20944/preprints202602.0471.v1

optimization, so as to achieve the improvement of the overall operational efficiency and emission reduction benefits of the road network.

Author Contributions: Conceptualization, Y.T.; Methodology, F.G.; Supervision, Y.L.; Writing—review & editing, F.G. All authors have read and agreed to the published version of the manuscript.

Funding: This research was supported by the Scientific Research Startup Fund Project of Fujian University of Technology (No. GY-Z23242) and the General Project of Young and Middle-aged Teachers' Educational and Scientific Research Project (Science and Technology Category) of Fujian Provincial Department of Education (No. JAT231055GY-Z23252).

Institutional Review Board Statement: Not applicable.

Informed Consent Statement: Not applicable.

Data Availability Statement: The data presented in this study are available on request from the corresponding author.

Acknowledgments: The authors acknowledge the support from the relevant highway operation entities in the Guangxi section.

Conflicts of Interest: The authors declare no conflict of interest.

Abbreviations

The following abbreviations are used in this manuscript:

VSL	Variable Speed Limit
MPC	Model Predictive Control
CFC	Car-Following Control
NSGA-II	The non-dominated sorting genetic algorithm

References

1. Lyu, P., Wang, P. S., Liu, Y., & Wang, Y. (2021). Review of the studies on emission evaluation approaches for operating vehicles. Journal of Traffic and Transportation Engineering (English Edition), 8(4), 493-509.Author 1, A.; Author 2, B. Title of the chapter. In *Book Title*, 2nd ed.; Editor 1, A., Editor 2, B., Eds.; Publisher: Publisher Location, Country, 2007; Volume 3, pp. 154–196. https://doi.org/10.1016/j.jtte.2021.07.004
2. Ravi, S. S., Osipov, S., & Turner, J. W. (2023). Impact of modern vehicular technologies and emission regulations on improving global air quality. Atmosphere, 14(7), 1164. https://doi.org/10.3390/atmos14071164
3. Allaby, P., Hellinga, B., & Bullock, M. (2007). Variable speed limits: Safety and operational impacts of a candidate control strategy for freeway applications. IEEE Transactions on Intelligent Transportation Systems, 8(4), 671-680. DOI: 10.1109/TITS.2007.908562
4. Fang, X., Péter, T., & Tettamanti, T. (2023). Variable speed limit control for the motorway–urban merging bottlenecks using multi-agent reinforcement learning. Sustainability, 15(14), 11464. https://doi.org/10.3390/su151411464
5. Han, Y., Wang, M., He, Z., Li, Z., Wang, H., & Liu, P. (2021). A linear Lagrangian model predictive controller of macro-and micro-variable speed limits to eliminate freeway jam waves. Transportation research part C: emerging technologies, 128, 103121. https://doi.org/10.1016/j.trc.2021.103121
6. Chen, D., & Ahn, S. (2015). Variable speed limit control for severe non-recurrent freeway bottlenecks. Transportation Research Part C: Emerging Technologies, 51, 210-230. https://doi.org/10.1016/j.trc.2014.10.015
7. Hegyi, A., & Hoogendoorn, S. P. (2010, September). Dynamic speed limit control to resolve shock waves on freeways-Field test results of the SPECIALIST algorithm. In 13th International IEEE Conference on Intelligent Transportation Systems (pp. 519-524). IEEE. DOI: 10.1109/ITSC.2010.5624974

 doi:10.20944/preprints202602.0471.v1

8. Hegyi, A., De Schutter, B., & Hellendoorn, J. (2005). Optimal coordination of variable speed limits to suppress shock waves. IEEE Transactions on intelligent transportation systems, 6(1), 102-112. DOI: 10.1109/TITS.2004.842408
9. Wang, M., Daamen, W., Hoogendoorn, S. P., & Van Arem, B. (2016). Connected variable speed limits control and car-following control with vehicle-infrastructure communication to resolve stop-and-go waves. Journal of Intelligent Transportation Systems, 20(6), 559-572. https://doi.org/10.1080/15472450.2016.1157022
10. Li, Z., Liu, P., Xu, C., Duan, H., & Wang, W. (2017). Reinforcement learning-based variable speed limit control strategy to reduce traffic congestion at freeway recurrent bottlenecks. IEEE transactions on intelligent transportation systems, 18(11), 3204-3217. DOI: 10.1109/TITS.2017.2687620
11. Han, Y., Hegyi, A., Yuan, Y., Hoogendoorn, S., Papageorgiou, M., & Roncoli, C. (2017). Resolving freeway jam waves by discrete first-order model-based predictive control of variable speed limits. Transportation Research Part C: Emerging Technologies, 77, 405-420. https://doi.org/10.1016/j.trc.2017.02.009
12. Mao, P., Ji, X., Qu, X., Li, L., & Ran, B. (2022). A variable speed limit control based on variable cell transmission model in the connecting traffic environment. IEEE Transactions on Intelligent Transportation Systems, 23(10), 17632-17643. DOI: 10.1109/TITS.2022.3160374
13. Vrbanić, F., Gregurić, M., Miletić, M., & Ivanjko, E. (2023). Reinforcement learning-based dynamic zone positions for mixed traffic flow variable speed limit control with congestion detection. Machines, 11(12), 1058. https://doi.org/10.3390/machines11121058
14. Li, Y., Pan, B., Chen, Z., & Xing, L. (2023). Developing a dynamic speed control system for mixed traffic flow to reduce collision risks near freeway bottlenecks. IEEE Transactions on Intelligent Transportation Systems, 24(11), 12560-12581. DOI: 10.1109/TITS.2023.3287269
15. Zhu, F., & Ukkusuri, S. V. (2014). Accounting for dynamic speed limit control in a stochastic traffic environment: A reinforcement learning approach. Transportation research part C: emerging technologies, 41, 30-47. https://doi.org/10.1016/j.trc.2014.01.014
16. Ke, Z., Li, Z., Cao, Z., & Liu, P. (2020). Enhancing transferability of deep reinforcement learning-based variable speed limit control using transfer learning. IEEE Transactions on Intelligent Transportation Systems, 22(7), 4684-4695. DOI: 10.1109/TITS.2020.2990598
17. Han, L., Zhang, L., & Pan, H. (2025). Improved multi-agent deep reinforcement learning-based integrated control for mixed traffic flow in a freeway corridor with multiple bottlenecks. Transportation Research Part C: Emerging Technologies, 174, 105077. https://doi.org/10.1016/j.trc.2025.105077
18. Khondaker, B., & Kattan, L. (2015). Variable speed limit: A microscopic analysis in a connected vehicle environment. Transportation Research Part C: Emerging Technologies, 58, 146-159. https://doi.org/10.1016/j.trc.2015.07.014
19. Coppola, A., Di Costanzo, L., Pariota, L., & Bifulco, G. N. (2023). Fuzzy-based variable speed limits system under connected vehicle environment: A simulation-based case study in the city of naples. IEEE Open Journal of Intelligent Transportation Systems, 4, 267-278. DOI: 10.1109/OJITS.2023.3266267
20. Roncoli, C., Papageorgiou, M., & Papamichail, I. (2015). Traffic flow optimisation in presence of vehicle automation and communication systems–Part II: Optimal control for multi-lane motorways. Transportation Research Part C: Emerging Technologies, 57, 260-275. https://doi.org/10.1016/j.trc.2015.05.011
21. Wu, Y., Tan, H., Qin, L., & Ran, B. (2020). Differential variable speed limits control for freeway recurrent bottlenecks via deep actor-critic algorithm. Transportation research part C: emerging technologies, 117, 102649. https://doi.org/10.1016/j.trc.2020.102649
22. Fondzenyuy, S. K., Turner, B. M., Burlacu, A. F., Jurewicz, C., Usami, D. S., Feudjio, S. L. T., & Persia, L. (2024). The Impact of Speed Limit Change on Emissions: A Systematic Review of Literature. Sustainability, 16(17), 7712. https://doi.org/10.3390/su16177712
23. Ma, C., Guo, J., & Zhao, Y. (2023). Variable speed limit control strategy at the entrance and exit of freeway tunnel. Physica A: Statistical Mechanics and its Applications, 632, 129292. https://doi.org/10.1016/j.physa.2023.129292

 doi:10.20944/preprints202602.0471.v1

24. Jin, J., Huang, H., Li, Y., Dong, Y., Zhang, G., & Chen, J. (2025). Variable speed limit control strategy for freeway tunnels based on a multi-objective deep reinforcement learning framework with safety perception. Expert Systems with Applications, 267, 126277. https://doi.org/10.1016/j.eswa.2024.126277
25. Jin, J., Li, Y., Huang, H., & Dai, J. (2025). A Connected-Automated Vehicles-Based Dynamic Speed Limit Control Strategy for Improving Safety and Efficiency of Freeway Tunnels: An Augmented Lagrange Safe Reinforcement Learning Framework. IEEE Internet of Things Journal. DOI: 10.1109/JIOT.2025.3535582
26. Csikós, A., Luspay, T., & Varga, I. (2011). Modeling and optimal control of travel times and traffic emission on freeways. IFAC Proceedings Volumes, 44(1), 13058-13063. https://doi.org/10.3182/20110828-6-IT-1002.01958
27. Zhai, Z., Tu, R., Xu, J., Wang, A., & Hatzopoulou, M. (2020). Capturing the variability in instantaneous vehicle emissions based on field test data. Atmosphere, 11(7), 765. https://doi.org/10.3390/atmos11070765
28. Liu, S., Li, H., Kun, W., Zhang, Z., & Wu, H. (2022). How do transportation influencing factors affect air pollutants from vehicles in China? Evidence from threshold effect. Sustainability, 14(15), 9402. https://doi.org/10.3390/su14159402
29. Ramadan, I., El Toukhy, M., Hussien, K. Z., Tosti, F., & Shaaban, I. G. (2022). Effect of road, environment, driver, and traffic characteristics on vehicle emissions in Egypt. International Journal of Civil Engineering, 20(11), 1261-1276.
30. Du, X., Kang, X., Gao, Y., & Wang, X. (2024). Driving behavior characterization and traffic emission analysis considering the vehicle trajectory. Frontiers in psychology, 14, 1341611. https://doi.org/10.3389/fpsyg.2023.1341611
31. Ning, Y., Sun, R., Hitchcock, D., Comert, G., & Chen, Y. (2025). Bayesian modeling of traffic-related air pollutants: A case study of urban transportation and air quality dynamics in Columbia, South Carolina. Atmospheric Environment: X, 100328. https://doi.org/10.1016/j.aeaoa.2025.100328